JOURNAL OF MATERIALS SCIENCE 26 (1991) 669–677

Nitridation reactions of molten Al–(Mg, Si) alloys

H. SCHOLZ, P. GREIL
Arbeitsbereich Technische Keramik, Technische Universität Hamburg-Harburg, D-2100 Hamburg 90, FRG

The isothermal nitridation of magnesium- and silicon-doped aluminium melt at 1273 K was investigated. With increasing Mg/Si ratio and decreasing oxygen content in the nitriding atmosphere, four major reaction mechanisms may be separated: (i) a passivating surface nitridation, (ii) a volume nitridation with precipitation of isolated AlN in the aluminium matrix, (iii) a volume nitridation resulting in a three-dimensionally interconnected AlN/Al composite microstructure, and (iv) a break-away nitridation with complete conversion of aluminium to AlN. The behavioural transition of the nitridation mechanism is reflected by the growth direction and the crystal morphology of AlN which change from inward (mechanisms i, ii) to outward (mechanisms iii, iv) growth of the reaction product with [0 0 0 1] as the dominating growth direction. Attempts are made to define the critical magnesium and silicon contents for the regime of controlled AlN/Al composite growth (mechanism iii) at 1273 K, in order to develop novel AlN/Al composite materials.

1. Introduction

Pure aluminium is known to be very resistant to oxidation, when exposed to air. A protective oxide film immediately generates on the surface even at low temperatures (specific volume ratio $V_{Al_2O_3}/V_{Al} = 1.28$), which prevents further oxidation of aluminium in the solid as well as in the liquid state, if the melt is undisturbed [1, 2]. In contrast to the passivation effect of dense surface layers, a surface active oxidation was observed in certain aluminium alloys which is characterized by a continuously growing porous oxide layer. Unexpected high oxidation rates were observed in magnesium-doped aluminium melts at reaction temperatures of 1173 to 1673 K, which were explained by an oxidation mechanism of magnesium, forming a non-protective, porous MgO or $MgAl_2O_4$ layer on the surface ($V_{MgO}/V_{Mg} = 0.81$) [1, 3–5]. Based on the enhanced oxidation behaviour of liquid aluminium alloys, a novel fabrication process of Al_2O_3/Al ceramic–metal composites (CMC), called directed melt oxidation (DIMOX), was developed [6]. High reaction rates at low reaction temperatures make this process particularly interesting for matrix formation in fibre-, whisker- or platelet-reinforced composite materials [7]. The unique microstructure is characterized by a three-dimensional interlocking of the continuous ceramic and metal phases, resulting in good strength, toughness and fatigue resistance even at temperatures up to the melting point of the metal phase [8]. Two types of alloying elements are necessary to stimulate an outward growth of the Al_2O_3/Al product: (i) initiator dopants such as magnesium to start the reaction, and (ii) surface active dopants such as silicon, germanium, tin or lead to improve wetting of the liquid alloy, in order to facilitate its transport through the reaction product to the reaction front. Activation energies of about 400 kJ mol^{-1} were found for the directed melt oxidation (DIMOX) with reaction rates of about 2×10^{-5} g cm^{-2} sec^{-1} at 1423 K [9].

In contrast to the increasing number of investigations on Al_2O_3/Al composite formation, only a few works have yet been concerned with the fabrication of AlN/Al composites. As with the oxidation, a protective surface layer ($V_{AlN}/V_{Al} = 1.26$) should form. In addition the very small solubility of nitrogen in aluminium (2×10^{-6} at % N at 1273 K [10]) points to a parabolic diffusion-controlled surface nitridation. By means of high-pressure metallurgy the solubility of nitrogen in liquid aluminium is increased, resulting in a homogeneous precipitation of AlN in aluminium upon cooling [11–13]. Three different reaction mechanisms were postulated for the dependence of temperature, nitrogen pressure and magnesium content of the alloy [13, 14]: (i) a surface reaction mechanism, forming a dense nitride layer on the melt surface, (ii) a volume reaction mechanism with the AlN reaction product as a dispersed phase in aluminium, (iii) a heterogeneous combustion mechanism with total conversion of aluminium to AlN.

In correspondence to the oxidation, magnesium is assumed to exert a catalytic effect on the nitridation of aluminium, i.e. to avoid the formation of a dense nitride layer and to transfer surface reaction to a volume reaction. In contrast to the surface nitridation, the volume nitridation proceeds internally in the bulk of the molten metal according to a solution-precipitation or (vapour–liquid–solid) VLS mechanism [14].

0022–2461/91 $03.00 + .12

High-purity AlN can be prepared by complete nitridation of molten Mg–Al alloys [15] and Zn–Al alloys [16] at temperatures above the boiling points of magnesium and zinc, 1363 and 1180 K, respectively, where the reaction product of these species is depleted. This method represents an alternative way to other important AlN production routes such as carbothermal reduction of alumina, directed nitridation of solid aluminium particles and nitridation of decomposed aluminium halides [17].

While the conditions for the DIMOX process to form Al_2O_3/Al composites are well defined [6], AlN/Al composites of similar microstructure may also be formed; the specific conditions, however, are not yet fully understood [18]. In particular, the influence of alloying elements and impurities in the nitriding atmosphere may be different to the oxidation. In contrast to earlier work [13, 14], a recent study on the nitridation of molten aluminium showed the effect of magnesium as a single dopant on aluminium nitridation to be poor, whereas Al(Mg, Si) alloys show very fast and complete nitridation behaviour [19]. The Al(Mg, Si) alloys used in this work, however, contained additional elements such as iron, zinc and copper, in concentrations up to 3.1 wt %. Zinc, especially, was reported to promote the oxidation of the aluminium melt [20]. Very slow heating rates of 4 K min^{-1} were applied in this study [19], so that any induction period, which is characteristic for melt oxidation and nitridation, could not be considered. In contrast to the melt oxidation, the activation energies of nitridation are four times lower ($\Delta E_A \sim 100$ kJ mol^{-1}) and the reaction rates at 1423 K were found to be three magnitudes higher (3×10^{-2} g cm^{-2} sec^{-1}) [18]. With increasing reaction rate, the residual porosity of the AlN/Al reaction product was also found to be significantly increased.

The aim of the present work was to investigate the combined influence of magnesium and silicon as alloying elements and the effect of oxygen impurities in the nitriding atmosphere on the isothermal aluminium nitridation reaction mechanism. The reaction kinetics and microstructure formation were analysed by means of thermal balance experiments, X-ray diffraction, optical and scanning electron microscopy. Thermodynamic calculations are used to discuss the behavioural transition of the different reaction mechanisms.

2. Experimental procedure

Various compositions of Al(Mg, Si) alloys were prepared by Vereinigte Aluminium-Werke AG (VAW, Bonn, FRG) and Alusuisse-Deutschland (Alusuisse, Konstanz, FRG), Table I. Cylinders, 15 mm diameter and 10 mm thick, were machined, ultrasonically cleaned in acetone and placed into alumina crucibles. The nitridation was performed in two different types of alumina tube furnace: (i) a resistance-heated high-temperature furnace (Heraeus, Hanau, FRG) with flowing atmosphere (0.2 l min^{-1} after 20 min purging with nitrogen), and (ii) a modified resistance-heated furnace (Hochtemperaturtechnik, Saarbrücken, FRG) with a programmable supply of two different gases in a static atmosphere. The temperature was controlled by a Pt/Pt–10%Rh thermocouple positioned directly above the samples. The furnace was evacuated (< 1 mbar, < 100 Pa) and refilled with nitrogen three times at 423 K to purify the atmosphere. In both furnaces the reaction gas was high-purity nitrogen (99.999%, major impurities H_2O < 5 v.p.m., O_2 < 3 v.p.m.).

The effect of oxygen in the atmosphere on the nitridation reaction was investigated by mixing oxygen (up to 3%) with the nitrogen reaction gas. Low oxygen contents (< 1 v.p.b.) were achieved by adding forming gas (5% H_2 in nitrogen). The amount of oxygen in the reaction gas (down to 0.1 v.p.m.) was measured by means of an oxygen analyser (Simac DS 2500, Blankenbach, FRG). All samples were heated with 5 K min^{-1} to 1273 K and held at this temperature for 15 h. From the weight change of the samples the extent of nitridation, e.g. the conversion ratio, α,

TABLE I Composition of aluminium alloys

Specimen	Elements (wt %)								Mg/Si
	Mg	Si	Zn	Cu	Ti	Fe	Mn	Al	
5N	–	–	–	–	–	–	–	99.999	0
1	0.001	5.0	0.004	0.001	–	–	–	bal.	0.0002
2	< 0.02	10.2	< 0.07	< 0.03	< 0.07	< 0.3	–	bal.	0.0002
3	0.4	9.5	< 0.07	0.01	0.05	0.15	0.05	bal.	0.042
4	0.6	5.5	< 0.07	< 0.03	< 0.07	< 0.03	–	bal.	0.11
5	1.25	0.015	–	–	–	–	–	bal.	83.3
6	2.05	0.81	–	–	–	–	–	bal.	2.53
7	2.14	0.15	–	–	–	–	–	bal.	14.3
8	2.5	0.029	0.005	0.001	–	–	–	bal.	86.2
9	2.5	10.2	< 0.07	< 0.03	< 0.07	< 0.03	–	bal.	0.25
10	2.5	14.5	< 0.07	< 0.03	< 0.07	< 0.03	–	bal.	0.17
11	2.65	0.105	–	–	–	–	–	bal.	25.2
12	3.0	0.45	< 0.3	< 0.15	< 0.2	< 0.5	–	bal.	6.67
13	3.0	4.85	–	–	–	–	–	bal.	0.62
14	3.1	1.1	< 0.05	< 0.01	< 0.2	< 0.15	< 0.4	bal.	2.82
15	5.2	1.2	< 0.05	< 0.01	< 0.2	< 0.15	< 0.4	bal.	4.33
16	8.79	12.35	–	–	–	–	–	bal.	0.71
17	10.61	0.42	–	–	–	–	–	bal.	25.2

was determined. The conversion ratio was calculated according to the reaction

$$2Al + xSi + yMg + N_2 \rightarrow 2AlN + xSi - yMg \quad (1)$$

$$\alpha = M_{Al}/M_N[m_{rp} - (m_{Al} + m_{Si})]/m_{Al} \quad (2)$$

where M denotes the molecular and m the actual weight of the indexed elements aluminium, nitrogen and silicon, and the reaction product, rp. Magnesium was assumed to evaporate from the specimen and precipitate after gas-phase reaction in the furnace tube, forming either MgO or Mg_3N_2 dependent on the oxygen content in the atmosphere. Only small amounts of magnesium were found on the sample surfaces, which were neglected in the calculation. Silicon was supposed to remain in the aluminium solution but to exert no influence on weight balance during nitridation at 1273 K. Complete conversion ($\alpha = 1$) of aluminium to AlN corresponds to a total weight gain of 52%.

The isothermal reaction rate $d\alpha/dt$ was evaluated from thermogravimetrical data at 1273 K (STA 409, Netzsch, Selb, FRG). Cylindrical TGA samples (diameter = 5.5 mm, h = 5 mm) were prepared and ultrasonically cleaned in acetone. The reaction gas was high-purity nitrogen and the flow rate was 0.03 l min^{-1}. Before each TGA run the specimen chamber was purified by evacuation (< 1 mbar, < 100 Pa). The heating rate up to 1273 K was 15 K min^{-1} and temperature was measured with a Pt/Pt–10% Rh thermocouple (± 0.3 K).

Crystalline phases in the reaction product were identified by means of X-ray powder diffraction using monochromatic Cu$K\alpha$ radiation (PW 1729, Philips, Netherlands). Optical microscopy and SEM were used to take micrographs from as-grown, polished and fractured surfaces, respectively. EDS was used to analyse the distribution of magnesium and silicon in the reaction product.

Thermodynamic calculations were carried out in order to predict the equilibrium compositions when the alloys were nitrided at 0.1 MPa N_2 with oxygen contents from 1 down to 10^{-5}%. The program equiTherm (VCH Verlagsgesellschaft mbH, Weinheim, FRG) [21] which is based on the SOLGASMIX program [22] calculates the equilibrium composition of condensed and gas-phase mixtures based on the method of free-energy minimization. Ten gaseous and eight condensed phases in the system Al–Mg–Si–O–N were considered in the calculations, the thermodynamic data of which are given in Table II [23, 24]. The results of the phase calculations are presented as isothermal Pourbaix diagrams of a special bulk composition showing the proportions of condensed phases in a mixture for a range of oxygen concentrations in the nitrogen atmosphere. To account for the presence of residual metal in the reacted product, the conversion ratio of initial aluminium content was restricted to 0.9, so that kinetic hindrance of complete nitridation reaction was simulated.

3. Results

3.1. Microstructure formation

The microstructure formation of the reaction product was found to be strongly influenced by the alloy and the atmosphere compositions. Based on the experimental data of the isothermal conversion of aluminium to AlN from 18 different Al–Mg–Si compositions in flowing nitrogen (~ 100 v.p.m. O_2) after 15 h at 1273 K the tentative diagram shown in Fig. 1 was established by interpolation between the measured data. In the absence of magnesium the nitridation of high-purity aluminium (99.999%) and Al–Si alloys was restricted to the formation of a thin protective AlN or Al_2O_3 layer on the surface, which prevented any further nitridation. A slight weight loss, < 0.6 wt %, indicated some aluminium volatilization. With increasing magnesium content, no passivating surface layer was formed, but a volume nitridation occurs with the reaction kinetics and microstructure of the product being strongly dependent on the silicon content in the alloy. Thus, magnesium evidently shows an initiating and accelerating effect on the nitridation kinetics, whereas silicon seems to exert an inhibiting character.

The nitridation of low-alloyed aluminium (Mg < 1 wt%), with an Mg/Si ratio of < 0.5, results in an Al/AlN reaction product of less than 2 mm thick, extending from the surface into the metal. The conversion of aluminium to AlN does not exceed 10%. Optical micrographs of the nitrided region show the AlN crystals uniformly dispersed in the metal matrix. In regions of high residual aluminium content, porosity is very low and AlN is of needle-like morphology,

TABLE II Gibbs energies at 1273 K [23]

Condensed species	G^0(kJ mol^{-1})	Gaseous species	G^0 (kJ mol^{-1})
Al	− 60.300	Al	101.826
AlN	− 378.607	Al_2O	− 507.336
Al_2O_3	− 1831.495	Mg	− 60.957
Mg	− 65.876	MgO[a]	− 248.627
Mg_3N_2	− 674.494	MgN[a]	− 28.193
MgO	− 674.747	N_2	− 270.170
$MgAl_2O_4$	− 2532.776	NO	− 205.087
Si	− 44.236	O_2	− 288.617
		Si	+ 217.429
		SiO	− 398.103

[a]Data from [24].

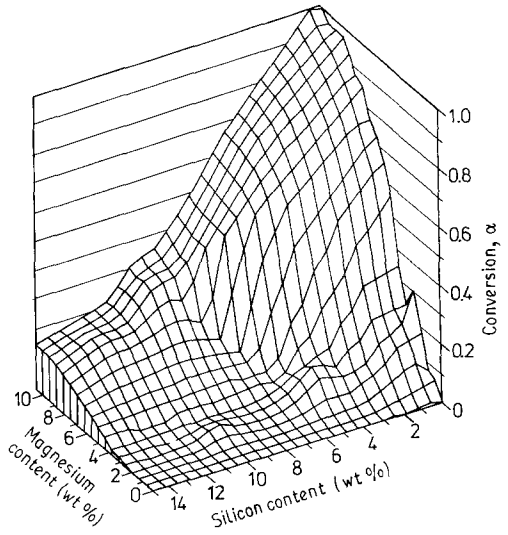

Figure 1 Conversion, α, of aluminium to AlN as a function of magnesium and silicon content after isothermal nitridation for 15 h at 1273 K in flowing nitrogen of 0.1 MPa (0.2 l min^{-1}, O_2 ~ 100 v.p.m.).

Fig. 2a. X-ray diffraction (XRD) analysis only revealed aluminium and AlN. SEM and energy dispersive spectroscopy (EDS) showed small amounts of silicon precipitations, which are uniformly segregated in the residual metal phase. While the residual metal was found to be depleted of magnesium, elevated magnesium concentrations were determined on the surface of the samples, which may be explained by the condensation of MgO.

Alloys with intermediate magnesium content (2 wt % < Mg < 4 wt %) and preferential silicon contents < 5 wt %, revealed a different nitridation behaviour with increased conversion to AlN up to 50 %. The reaction product grows in the opposite direction towards the gas phase, as is typical for the DIMOX process [6]. The reaction product consists of aluminium and AlN both three-dimensionally interconnected with silicon sparsely segregated in the aluminium phase, Fig. 2b. Increased conversion to AlN resulted in increased porosity, although the specific volume ratio of AlN/Al is 1.26 [25].

In contrast to the controlled nitridation which results in an Al/AlN composite microstructure, a further mechanism occurs in highly magnesium-doped alloys (Mg > 4 wt %) with Mg/Si > 10. The inhibiting influence of small amounts of silicon is not sufficient to counteract the accelerating effect of magnesium. A break-away reaction occurs resulting in up to 100% conversion of aluminium to AlN. While the surface of the reaction product shows a black colour covered with a thin white layer, the bulk consists of friable white and needle-like grains, Fig. 2c. The white deposit was identified by X-ray analysis to be MgO, whereas the pulverized bulk product, crushed in an agate mortar was found to be pure AlN. XRD analysis of the as-grown black nitride surface only showed the (0 0 0 2) and (0 0 0 4) peaks, which evidently determines the *c*-axis as the dominating growth direction. The [0 0 0 1] growth of AlN perpendicular to the surface was also found in a recent work [9].

In order to study the effect of small oxygen contents in the reaction gas, hydrogen or oxygen, was admixed to the nitrogen. Fig. 3 shows the conversion ratio of alloy 6 after 15 h at 1273 K in static nitrogen atmosphere containing 0.7 vol % H_2, 3×10^{-4}, 1.3 and 3.1 vol % O_2, respectively. With increasing oxygen content the conversion of aluminium to AlN is significantly reduced. Evaporated magnesium reacted with oxygen forming solid MgO, which was found precipitated as a white deposit on the sample surface, the crucible walls and in the furnace. Hydrogen additions

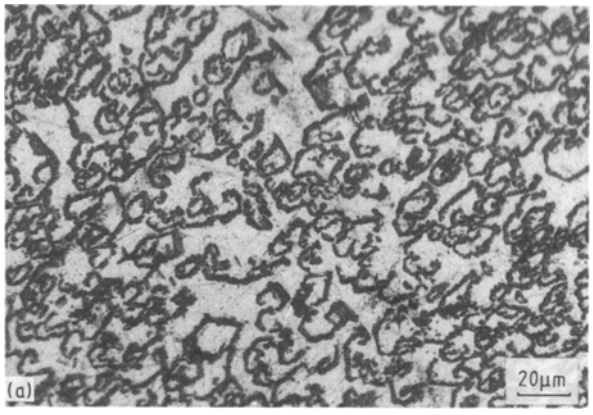

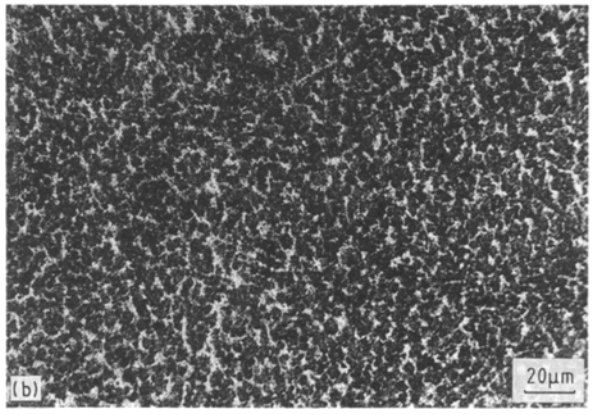

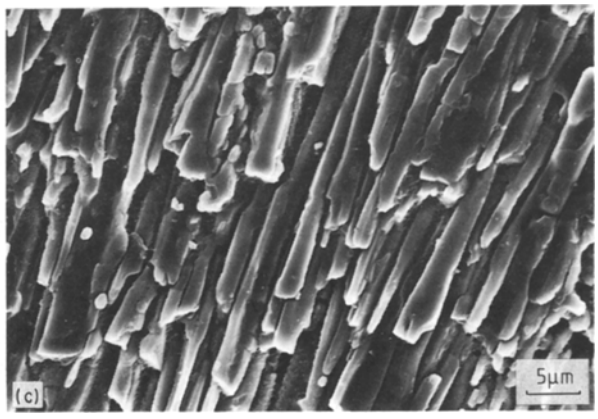

Figure 2 (a) Microstructure of specimen 5 representing nitridation mechanism ii with low conversion α = 0.063 (optical micrograph, polished surface). (b) Microstructure of specimen 12 representing nitridation mechanism iii with controlled outward growth of a porous AlN/Al product and a local conversion of about α ~ 0.5 (optical micrograph, polished surface). (c) Microstructure of specimen 17 representing nitridation mechanism iv with break-away nitridation and fully conversion α = 1 (scanning electron micrograph, fracture surface).

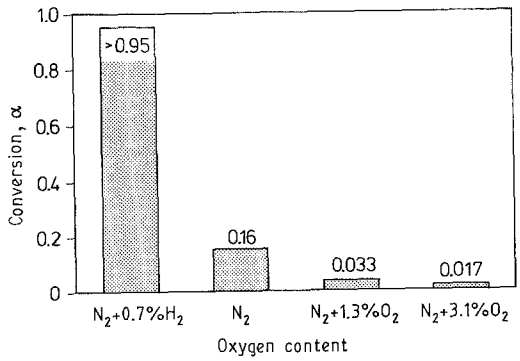

Figure 3 Conversion, α, of specimen 6 after isothermal nitridation at 1273 K for 15 h as a function of the initial oxygen or hydrogen content in the static nitrogen atmosphere.

to the nitrogen resulted in precipitation of finely dispersed magnesium in the furnace tube. Neither MgO, nor Mg_3N_2 was detected. The conversion to AlN was complete and the samples showed enhanced aluminium wetting of the crucible walls and break away nitridation.

3.2. Reaction kinetics

High magnesium contents in the aluminium alloy resulted in an acceleration of the reaction rate. Fig. 4a shows the isothermal weight change of specimens 8 and 6 at 1273 K in flowing nitrogen containing < 0.1 v.p.m. O_2. While specimen 8 (Mg/Si = 86.2) was completely converted to AlN ($\alpha = 1$) within 200 min, specimen 6 required more than 600 min to attain a conversion ratio of $\alpha \sim 0.5$. Fig. 4b shows the reaction rates $d\alpha/dt$ plotted against the reaction time $t - t_0$, where t_0 is the time when measurable weight gain started. As may be seen from both figures, the nitridation reaction kinetics can be separated into an incubation period with slowly increasing reaction rate and a successive period with rapid conversion. For $t \geq t_0$ the reaction rates were analysed according to the relation

$$d\alpha/dt = k(T)f(\alpha) \quad (3)$$

where $k(T)$ expresses the temperature and $f(\alpha)$ the concentration dependence of the reaction rate under isothermal conditions [26]. For specimen 8 the reaction rate data were found to be best fitted by

$$f(\alpha) = (1 - \alpha)\alpha \quad (4)$$

with a correlation coefficient of $R = 0.997$. Specimen 6 may be well described with the same relation at the initial period $\alpha = 0$ to 0.3 with $R = 0.994$. Both the measured and calculated curves are given in Fig. 4b. Equation 4 describes a solid state reaction with an exponential nucleation followed by a linear growth of the reaction product [26, 27]. The final period of sample 6 may better be described by

$$f(\alpha) = 1/2\,\alpha^{-1} \quad (5)$$

($R = 0.994$), which represents a diffusion-controlled reaction [27].

4. Discussion

4.1. Influence of atmospheric composition

The results described above illustrate a complex nitridation behaviour of magnesium- and silicon-doped aluminium alloys. The transition of the nitridation mechanism with the atmospheric composition may be correlated to the results of the thermodynamic calculations. The equilibria composition of the resulting phase mixtures of pure aluminium, magnesium and the alloy Al–5Si–5Mg were calculated at 1273 K for oxygen contents of 1 to 10^{-5} vol % in the nitrogen atmosphere at 0.1 MPa. Although the calculations could not consider the effect of passivating layers and other kinetic hindrance, general trends of the phase formation at 1273 K can be derived. For the pure metals a threshold oxygen content in the nitrogen atmosphere exists, above which the oxide and below which the nitride becomes stable, according to the reaction

$$Al_2O_3 + N_2 \xrightarrow[p_{N_2}=1]{} 2AlN + \frac{3}{2}O_2 \quad (6)$$

for which the Gibb's energy of formation, $\Delta_f G^0 = +908.9\ kJ\,mol^{-1}$ at 1300 K [24]. The critical p_{O_2} is given as a function of the oxide and nitride activities

$$p_{O_2} = \left[\frac{a_{Al_2O_3}}{a_{AlN}^2}\exp\left(-\frac{\Delta_f G^0}{RT}\right)\right]^{2/3} \quad (7)$$

Thus, at 1273 K, pure aluminium is expected to be oxidized in a nitrogen atmosphere (0.1 MPa) down to $p_{O_2} \sim 10^{-20}$ Pa, Fig. 5. This was confirmed by the XRD and EDX analysis with an ultrathin beryllium window, which showed the formation of dense Al_2O_3 layers on the surface of the unreacted melt. Using

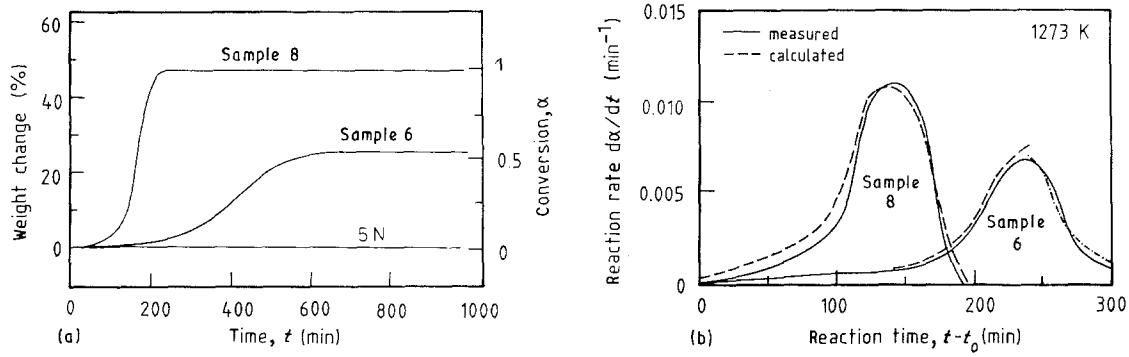

Figure 4 (a) Isothermal weight change at 1273 K in flowing nitrogen atmosphere (0.03 l min^{-1}, $O_2 < 0.1$ v.p.m.) of pure and magnesium-, silicon-alloyed aluminium melt; (b) reaction rates $d\alpha/dt$ after onset of weight gain at t_0, (——) measured, (– – –) calculated.

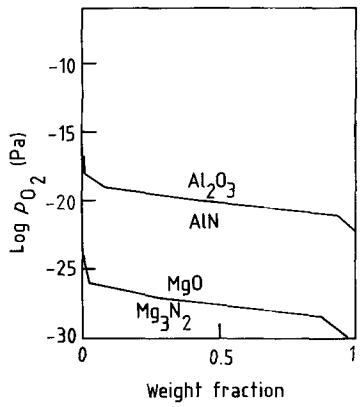

Figure 5 Isothermal Pourbaix diagram at 1273 K of the condensed phase mixtures of the systems Al–N–O and Mg–N–O, showing the stability regions as a function of the oxygen partial pressure in the nitriding atmosphere at 0.1 MPa.

similar expressions for metallic magnesium the phase stability diagram in Fig. 5 is obtained. In the presence of condensed magnesium in the reaction atmosphere, extremely low oxygen partial pressures of $p_{O_2} < 10^{-30}$ Pa are indicated by the Ellingham diagram of the MgO system [28], due to the reaction

$$Mg(l, g) + O_2(g) \rightarrow MgO(s, g) \quad (8)$$

Thus, when magnesium is used as an oxygen getter in the reaction system, the oxygen partial pressure may be reduced below the threshold value of Al_2O_3–AlN stability transformation, which is confirmed by the observation of a black AlN layer on aluminium.

In the magnesium- and silicon-doped alloys a volume reaction occurred when Mg > 1 wt %, the reaction rate and the conversion ratio being strongly influenced by the silicon content in the alloy and the oxygen content in the nitriding atmosphere. For extremely low p_{O_2}, Ellingham diagrams established for the systems Mg–O, Al–O and Si–O, show the ratio of the partial pressures of Mg:Al:Si vapour over condensed metals at 1273 K as $10^6:1:10^{-3}$ (assuming metal activity coefficients = 1) [28]. Thus, magnesium is considered to be the major vapour species over the alloy melt and the oxygen concentration in the atmosphere will be dominated by Reaction 8. Fig. 6a and b show the calculated equilibrium compositions of the condensed phases of an alloy composition Al–5Mg–5Si at 1273 K as a function of the oxygen content in the nitriding atmosphere. Fig. 6a represents static and Fig. 6b flowing atmosphere conditions, which were simulated in the calculation using a small (6.4 Al + 0.34 Si + 0.39 Mg + 10 $N_2(O_2)$) and a large (6.4 Al + 0.34 Si + 0.39 Mg + 4000 $N_2(O_2)$) excess of nitrogen, respectively. While silicon remains unaffected in the residual aluminium melt, which exhibits a solubility for silicon of approximately 43 wt % at 1273 K [29], magnesium strongly affects the equilibrium phase formation. Under a static atmosphere only AlN is formed as the aluminium reaction product at all oxygen contents < 1 %. AlN is predicted to be in equilibrium with MgO and Mg_3N_2 above an oxygen content of approximately 10^{-2} % but only with Mg_3N_2 at lower oxygen concentrations. In flowing nitrogen, however, Al_2O_3 will be the stable phase above a threshold value of oxygen, which is in equilibrium with $MgAl_2O_4$ and MgO as has been observed in the Al_2O_3/Al composite formation [30]. In contrast to the static atmosphere, significantly lower oxygen contents in the nitriding atmosphere are necessary to obtain AlN and Mg_3N_2 as the stable phase composition, as may be expected from the partial pressure generation of magnesium and its effect on the p_{O_2} [28]. This is confirmed by the experimental finding, that nitridation could easily be achieved in static, but required oxygen reduction in flowing nitrogen atmospheres.

Fig. 7a and b summarize the calculated partial pressures of the gaseous species over the condensed phases given in Fig. 6a and b. The calculation refers to equilibrium generation, which, however, will definitely not be reached in flowing atmosphere. Thus, the calculated partial pressures may only indicate the tendency of the response of the complex system to external changes of the atmospheric composition. In flowing atmosphere only a low p_{Mg} develops in the range of higher oxygen contents in the nitriding atmosphere, where no nitridation reaction could be observed. With decreasing oxygen content or in static atmospheric conditions the p_{Mg} increased to an equilibrium value and break-away nitridation with complete conversion from aluminium to AlN was observed even at low magnesium concentrations in the alloy.

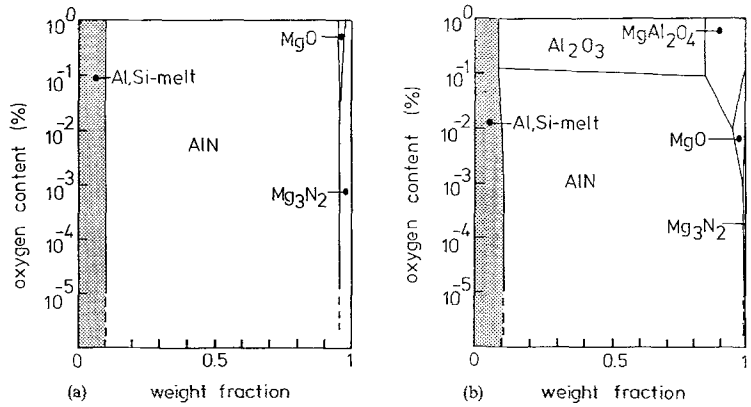

Figure 6 Isothermal Pourbaix diagrams at 1273 K of the condensed phase mixtures of the system Al–Mg–(Si)–N–O simulating (a) "static" and (b) "flowing" nitrogen atmosphere for an alloy composition Al–5Si–5Mg.

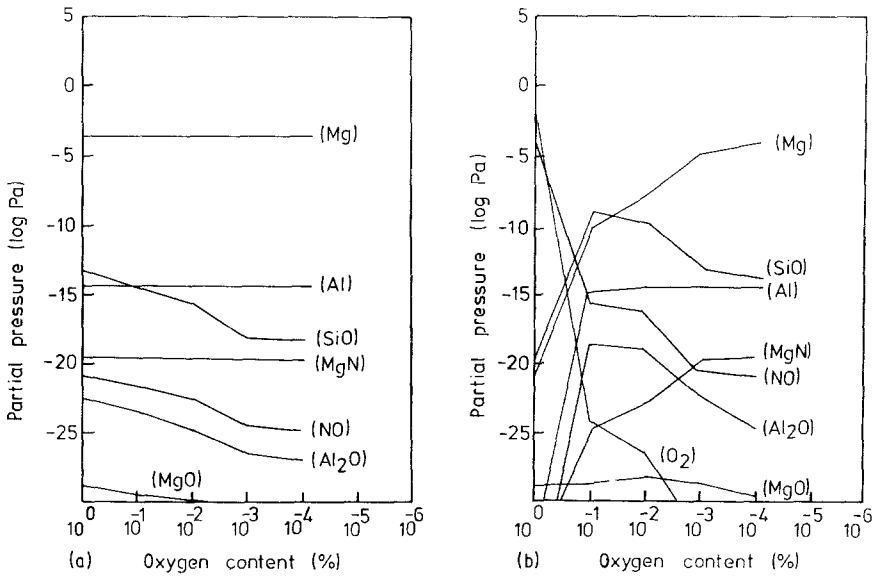

Figure 7 Partial pressures of the gaseous species at 1273 K over Al–5Si–5Mg calculated for (a) "static" and (b) "flowing" nitrogen atmosphere as a function of its oxygen content.

Although it is not yet clear whether the high magnesium volatility, the reduced specific volume of the initially formed Mg_3N_2 or MgO or the high heat of formation of both phases gives rise to the formation of a porous surface layer and hence for induction of outward growth of the reaction layer, the oxygen content in the nitrogen atmosphere exerts a strong influence on the phase formation in this system. Hence, by changing the nitriding atmospheric composition, volatilization of alloy elements and surface reactions may be controlled in order to optimize nitridation kinetics and microstructure formation.

4.2. Influence of alloy composition

On pure aluminium metal a dense AlN layer is immediately formed in a nitrogen atmosphere at 1273 K, which prevents further nitridation. The nitridation mechanism in this case is supposed to be controlled by the inward diffusion of nitrogen. Aluminium alloys containing low magnesium contents < 1 wt % only show a conversion of aluminium to AlN of $\alpha < 0.1$ and are characterized by the formation of reaction layers approximately 1 mm thick after 15 h nitridation. Thus, in magnesium-poor alloys the nitridation kinetics is supposed to be controlled by inward diffusion of nitrogen via the melt phase and subsequent precipitation of AlN. The AlN crystal morphology indicates a dendritic growth mechanism.

Aluminium alloys containing more than 2 wt % Mg are characterized by the outward growth of the AlN/Al reaction product towards the gas phase, as described for the DIMOX process [6]. Reaction rate data indicate that after an incubation period which may be related to the nucleation of the initial porous surface layer, the conversion proceeds by linear growth of AlN, until all aluminium is consumed or diffusion becomes dominant, due to reduced melt area in the growth product. A linear growth of hollow AlN crystals perpendicular to the initial melt surface can be seen in Fig. 8a and b. The aluminium melt may be transported to the reaction site via the open channels as observed for the directed melt oxidation [6] and also for the directed melt nitridation [18].

Nitridation of alloys with high magnesium contents and low silicon contents with Mg/Si > 10 resulted in very fast reaction rates after an incubation period, followed by full conversion to AlN. A mechanism involving vapour-phase reaction was believed to be responsible for this combustion-like nitridation [14]. Considering the extreme wetting behaviour in the first stage of nitridation, however, a liquid-phase reaction seems to be more reasonable. When nitridation was interrupted in an early stage at $\alpha < 0.08$ a very similar microstructure to that of mechanism ii (Fig. 2a) was observed. The very rapid nitridation may be attributed to an increased nitrogen uptake of the liquid alloy, because continuously fresh aluminium is exposed to the reaction gas during the wicking process. Break-away nitridation is provoked especially in a stationary forming-gas atmosphere and/or at elevated magnesium partial pressures, both resulting in very low p_{O_2} in the atmosphere. In a flowing atmosphere, only low p_{Mg} can be established (Fig. 7), because the volatilized magnesium is immediately carried away from the reaction site.

Summarizing the different mechanisms, an isothermal reaction map may be established, Fig. 9, which qualitatively shows the dependence of the type of nitridation on the Mg–Si content in the aluminium alloys. This map is generated from nitridation experiments at 1273 K and 0.1 MPa flowing nitrogen (0.2 l min^{-1}, $O_2 \sim 100$ v.p.m.). Four major reaction mechanisms may be separated: (i) a passivating surface nitridation, (ii) a volume nitridation with precipitation of isolated AlN in the aluminium matrix, (iii) a volume nitridation involving outward growth of an AlN/Al composite microstructure, and (iv) a break-away nitridation with complete conversion to AlN. With decreasing oxygen impurities, increasing temperature or increasing nitrogen pressure, the region of break-away nitridation is considerably enlarged. This is

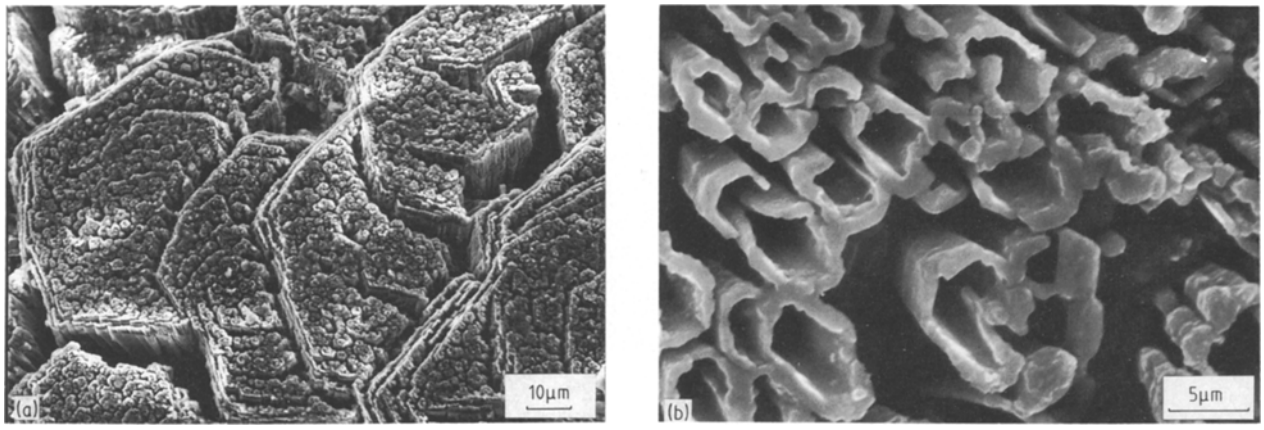

Figure 8 Scanning electron micrographs of (a) the etched growth surface and (b) a polished and etched (0.2% HF, 40 min) section of specimen 6 showing outward growth of hollow AlN crystals.

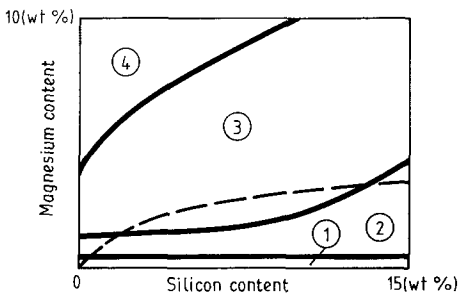

Figure 9 Tentative isothermal reaction map of Al–(Mg, Si) melt at 1273 K in flowing nitrogen (0.1 MPa, $O_2 \sim 100$ v.p.m.): (1) passivating surface nitridation, (2) diffusion-controlled volume nitridation, (3) volume nitridation involving outward growth of AlN/Al, (4) break-away nitridation; (– – –) oxygen contents $\ll 0.1$ v.p.m. with break-away nitridation (iv) above, and controlled nitridation (i to iii) below the dashed line.

demonstrated for extremely low oxygen contamination, $\ll 0.1$ v.p.m., in Fig. 9 by the dashed curve, separating break-away (iv) and controlled nitridation mechanisms (i–iii). An uncontrollable, complete conversion from aluminium to AlN occurs even at low magnesium concentrations in the alloy if the oxygen partial pressure is decreased by external oxygen getter materials in the furnace, such as magnesium, tantallum, zirconium, etc.

5. Conclusions

The fabrication of Al_2O_3/Al ceramic–metal composites by directed oxidation has led to interest in forming AlN/Al materials with similar microstructure. Controlled nitridation of aluminium, however, may only be obtained when a critical range of oxygen partial pressures in the atmosphere is not exceeded. The oxygen content is strongly dependent on the alloying elements, e.g. magnesium reduces the oxygen partial pressure to extremely low values. Thus, nitridation of aluminium is more sensitive to the atmospheric and alloy compositions as in oxidation, and requires careful control of reaction conditions. The oxygen content may be used as an external variable to change the nitridation mechanism during the reaction and hence microstructure formation. The silicon content may serve as an internal variable to control reaction kinetics. In particular, the reduction of the residual amount of aluminium in the AlN/Al composite microstructure may be achieved, so that the applicability of these materials at high temperatures will be improved.

Acknowledgements

Financial support of German Ministry for Science and Technology, BMFT-project no. 03M 10372, is gratefully acknowledged.

References

1. W. THIELE, *Aluminium* **38** (1962) 780.
2. W. HEHN and E. FROMM, *ibid.* **64** (1988) 180.
3. C. N. COCHRAN, D. L. BELITSKUS and D. L. KINOSZ, *Metall. Trans. B* **8** (1977) 323.
4. D. L. BELITSKUS, *Oxid. Metals* **3** (1971) 313.
5. N. B. PILLING and R. E. BEDWORTH, *J. Inst. Metals* **29** (1923) 529.
6. M. S. NEWKIRK, A. W. URQUHART, H. R. ZWICKER and E. BREVAL, *J. Mater. Res.* **1** (1986) 81.
7. M. S. NEWKIRK, H. D. LESHER, D. R. WHITE, C. R. KENNEDY, A. W. URQUHART and T. D. CLAAR, *Ceram. Engng Sci. Proz.* **8** (1987) 879.
8. M. K. AGHAJANIAN, N. H. MACMILLAN, C. R. KENNEDY, S. J. LUSZCZ and R. ROY, *J. Mater. Sci.* **24** (1989) 658.
9. A. S. NAGELBERG, presented at the 90th Annual Meeting of the American Ceramic Society", Cincinatti, Ohio, 1988 (Engineering Ceramics Division, paper no. 107-c-88).
10. H. A. WRIEDT, *Bull. Alloy Phase Diagrams* **7** (1986) 329.
11. F. ERDMANN-JESNITZER and M. YÜKSEL, *Metall.* **29** (1975) 341.
12. P. C. BORBE, F. ERDMANN-JESNITZER and E. J. JUN, *ibid.* **9** (1978) 884.
13. A. SCHWEIGHOFER and S. KUDELA, *Kovove Mater.* **3** (1977) 257.
14. S. KUDELA and A. SCHWEIGHOFER, 7th International Light Metals Congress, Leoben/Vienna, 22–26 June, 1981, (Aluminium Verlag, Düsseldorf 1981).
15. S. KUDELA and A. SCHWEIGHOFER, Cs. Pat. 189 513 (1978).
16. Ir. M. VAN DAM, Philips Gloeilampenfabrieken/Eindhoven, Pat. 6 602 899 (1966).
17. G. A. SLACK and T. F. MCNELLY, *J. Crystal Growth* **34** (1977) 482.
18. D. K. CREBER, S. D. POSTE, M. K. AGHAJANIAN and T D. CLAAR, *Ceram. Engng Sci. Proc.* **9** (1988) 975.

19. H. LEHUY and S. DALLAIRE, In "Proceedings of the International Symposium on Advances in Processing of Ceramic and Metal-Matrix Composites", Halifax, Canada, 20–24 August, 1989 (Pergamon, New York, 1989) p. 302.
20. M. DROUZY and M. RICHARD, *Fonderie* **322** (1974) 121.
21. M. ZEITLER, B. WITTIG, and W. SCHMIDT, "equiTherm", VCH Wissenschaftliche Software (1989).
22. G. ERIKSSON, *Chem. Scripta* **8** (1975) 100.
23. I. BARIN, "Thermochemical Data of Pure Substances" (VCH Verlagsgesellschaft, Weinheim, 1989).
24. "JANAF Thermochemical Tables", 3rd Edn, *J. Phys. Chem. Ref. Data*, **14** Suppl. 1 (1985).
25. F. L. RILEY, in "Nitrogen Ceramics", Proceedings of NATO Advanced Study Institute on Nitrogen Ceramics, 16–17 August 1976 (Noordhoff, 1977) p. 265.
26. J. SESTAK and G. BERGGREN, *Thermo-chim. Acta* **3** (1971) 1.
27. P. P. BUDNIKOV and A. M. GINSTLING, "Principles of Solid State Chemistry" (Gordon and Beach, New York, 1968) (translated from Russian).
28. V. L. K. LOU, T. E. MITCHELL the A. H. HEUER, *J. Amer. Ceram. Soc.* **68** (1985) 49.
29. J. L. MURRAY and A. J. McALISTER, *Bull. Alloy Phase Diagrams* **5** (1984) 74.
30. M. SINDEL, N. A. TRAVITZKY and N. CLAUSSEN, *J. Amer. Ceram. Soc.* **73** (1990) 2645.

Received 7 November 1989
and accepted 9 January 1990